

UNCLASSIFIED

AD NUMBER

AD323887

CLASSIFICATION CHANGES

TO: **UNCLASSIFIED**

FROM: **CONFIDENTIAL**

LIMITATION CHANGES

TO:

**Approved for public release; distribution is
unlimited.**

FROM:

**Distribution authorized to U.S. Gov't. agencies
and their contractors;
Administrative/Operational Use; 03 APR 1961.
Other requests shall be referred to Bureau of
Naval Weapons, Washington, DC.**

AUTHORITY

30 Apr 1973, DoDD 5200.10 ; NOL ltr 29 Aug 1974

THIS PAGE IS UNCLASSIFIED

UNCLASSIFIED

AD 323 887

*Reproduced
by the*

**ARMED SERVICES TECHNICAL INFORMATION AGENCY
ARLINGTON HALL STATION
ARLINGTON 12, VIRGINIA**



NOTICE: When government or other drawings, specifications or other data are used for any purpose other than in connection with a definitely related government procurement operation, the U. S. Government thereby incurs no responsibility, nor any obligation whatsoever; and the fact that the Government may have formulated, furnished, or in any way supplied the said drawings, specifications, or other data is not to be regarded by implication or otherwise as in any manner licensing the holder or any other person or corporation, or conveying any rights or permission to manufacture, use or sell any patented invention that may in any way be related thereto.

~~CONFIDENTIAL~~

NAVWEPS REPORT

7389

151300

323887

CATALOGED BY ASTIA
AS AD No. /

DRAG AND STABILITY DATA FOR SEVERAL SAMOS CONFIGURATIONS
OBTAINED FROM FREE-FLIGHT MODEL FIRINGS (C)

RELEASED TO ASTIA
BY THE NAVAL ORDNANCE LABORATORY

Without restrictions
 For Release to Military and Government Agencies Only.
 Approval by BuWeps required for release to contractors.
 Approval by BuWeps required for all subsequent release.

3 APRIL 1961



NOTICE: This material contains information affecting the national defense of the United States within the meaning of the Espionage Laws, Title 18, U.S.C., Sections 793 and 794, the transmission or revelation of which in any manner to an unauthorized person is prohibited by law.

U. S. NAVAL ORDNANCE LABORATORY
WHITE OAK, MARYLAND

XEROX

~~CONFIDENTIAL~~

DOWNGRADED AT 3 YEAR INTERVALS;
DECLASSIFIED AFTER 12 YEARS
DOD DIR 5200.10

ASTIA
REF ID: A
JUN 28 1961
TIPDR A

CONFIDENTIAL
NAVWEPS Report 7389

Ballistics Research Report 39

DRAG AND STABILITY DATA FOR SEVERAL SAMOS CONFIGURATIONS
OBTAINED FROM FREE-FLIGHT MODEL FIRINGS

Prepared by:

Leonard E. Crogan

ABSTRACT: Firings of several SAMOS configurations were conducted in the Naval Ordnance Laboratory Pressurized Ballistics Range No. 3. The configurations differed in nose corner radius only. It was observed that with a decrease in the nose corner radius, the drag coefficient increased, the slope of the normal force coefficient decreased, and the slope of the pitching moment coefficient increased. From these experimental data, it was concluded that a decrease in the nose corner radius resulted in a rearward movement of the center of pressure.

U. S. NAVAL ORDNANCE LABORATORY
WHITE OAK, MARYLAND

~~CONFIDENTIAL~~

CONFIDENTIAL

NAVWEPS Report 7389

3 April 1961

This report presents the results of firings made with models of the SAMOS configuration in the Naval Ordnance Laboratory's Pressurized Ballistics Range No. 3 to determine their free-flight characteristics.

This work was done at the request of the Research and Advanced Development Division of AVCO Corporation under task number AFO4-(647)347. Appreciation is extended to Miss Amy A. Chamberlin for reducing the data and to Mr. John E. Fontenot for his assistance in the firing of many models.

W. D. COLEMAN
Captain, USN
Commander

A. E. SEIGEL
By direction

¹¹
CONFIDENTIAL

CONFIDENTIAL
NAVWEPS Report 7389

CONTENTS

	Page
Introduction.....	1
Model Details.....	1
Discussion and Results.....	2
Conclusions.....	3
References.....	5

ILLUSTRATIONS

Table I	Average Weights and Moments of Inertia of SAMOS Models
Table II	Drag and Stability Data for SAMOS Models (Drawing No. 1831)
Table III	Drag and Stability Data for SAMOS Models (Drawing No. 1831-5)
Table IV	Drag and Stability Data for SAMOS Models (Drawing No. 1844)
Table V	Drag and Stability Data for SAMOS Models (Drawing No. 2304-11)
Table VI	Drag and Stability Data for SAMOS Models (Drawing No. 2205-5)
Table VII	Drag and Stability Data for SAMOS Models (Drawing No. 2304-7)
Table VIII	Drag and Stability Data for SAMOS Models (Drawing No. 2304-9)
Figure 1	SAMOS Models
Figure 2	SAMOS Models and Sabots
Figure 3	Shadowgraph Print of SAMOS Model with a Full-Scale Nose Corner Radius of Two Inches (1831-5), Round 3812, $M = 4.94$
Figure 4	Complex Angle of Attack Plots for SAMOS Models
Figure 5	Slope of Damping Moment Coefficient for SAMOS Models as a Function of Mach Number
Figure 6	Zero Yaw Drag Coefficient for SAMOS Models as a Function of Mach Number
Figure 7	Slope of Normal Force Coefficient Corrected to Zero Yaw for SAMOS Models as a Function of Mach Number
Figure 8	Slope of Pitching Moment Coefficient Corrected to Zero Yaw for SAMOS Models as a Function of Mach Number

CONFIDENTIAL
NAVWEPS Report 7389

SYMBOLS

$C_D = \frac{D_t}{qS}$ = total drag coefficient based on the maximum cross-sectional area(S) of the model

$C_{M\alpha} = (\text{slope of the pitching moment})/qSD$ = slope of the pitching moment coefficient referred to the CG

$C_{Mq} + C_{M\alpha} = (\text{slope of yaw damping moment due to } q)/(D/2V) qSD +$

$(\text{slope of yaw damping moment due to } \alpha)/(\frac{D}{2V}) qSD =$
slope of damping moment coefficient referred to the CG

$C_{N\alpha} = (\text{slope of normal force})/qS$ = slope of normal force coefficient

CG_N = center of gravity, subscript N denotes measured from nose of model

CP = center of pressure

D = maximum diameter of model

D_t = component of the aerodynamic force directed along the trajectory

I = moment of inertia about CG, I_A denotes axial and I_B , transverse

k_D , k_M , k_N = parameters used to correct to zero yaw the drag, pitching moment, and normal force coefficients, respectively (see paragraph 9 of the text)

M = Mach number (based on midrange value of V)

P.E. = probable error based on accuracy of data fitting
(P.E.s, swerve equation; P.E.y, yaw equation)

$q = \frac{\rho V^2}{2}$ = dynamic pressure or q = lateral component of angular velocity of model

$Re_D = \frac{\rho V D}{\mu}$ = Reynolds number based on maximum diameter (D) of model

$S = \frac{\pi D^2}{4}$ = maximum cross-sectional area of model

CONFIDENTIAL
NAVWEPS Report 7389

SYMBOLS

V = velocity (usually a midrange value)

α = angle of attack

$\dot{\alpha}$ = rate of change of angle of attack with time

δ^2 = mean squared yaw

μ = coefficient of viscosity

ρ = density of air

λ_1 , λ_2 = damping rates of nutational arm (1) and precessional arm (2)

Subscript

o coefficient corrected to zero yaw

V

CONFIDENTIAL

CONFIDENTIAL
NAVWEPS Report 7389

DRAG AND STABILITY DATA FOR SEVERAL SAMOS CONFIGURATIONS
OBTAINED FROM FREE-FLIGHT MODEL FIRINGS

INTRODUCTION

1. Models of several SAMOS configurations were fired in the Naval Ordnance Laboratory Pressurized Ballistics Range No. 3 (reference (a)) to determine their drag and stability characteristics. The configurations differed only in nose corner radius.

Model Details

2. Sketches are presented in Figure 1 of all of the SAMOS model configurations tested. Table I lists the average weights and moments of inertia of these configurations. Rounds 3846 and 3849 are listed separately from the rest of the rounds of their respective drawing numbers because they were manufactured of different materials from the rest of the rounds. This difference in material caused these rounds to differ from the rest of the rounds in weight and moment of inertia only.

3. Models of three different sizes were used. Their maximum diameters were 0.750, 0.600, and 0.500 inches. The configurations differed in nose corner radius only. Four different radii were investigated. The full-scale nose corner radii were one, two, five, and eight inches. Models of the configurations having either one-inch or eight-inch nose corner radius were tested with only one center of gravity location for each configuration. Models of the configurations having either two-inch or five-inch nose corner radius were tested with two center of gravity locations for each configuration.

4. Sabots to cradle the models at initial angles of 0, 10, 15, 20, and 25 degrees were used in launching the models. Figure 2 is a photograph of a model and sabot designed for launching the model at 25° from a powder gun and a model and sabot designed for launching the model at 0° from a light-gas gun.

5. Figure 3 is a shadowgraph of a model from drawing number 1831-5 in flight at a Mach number of 4.94.

Discussion and Results

6. The models were fired at the different initial launch angles to determine if the dynamic stability of the configurations is affected by angle of attack. The results of this program indicate that neither angle of attack nor any of the center of gravity locations investigated affected the dynamic stability of the configurations. This is graphically shown in Figure 4 where angle of yaw is plotted against pitching angle. The axes are in multiples of degrees as shown on each graph. The motion of the model starts where the two oversized dots are plotted. As can be seen, the maximum amplitude of the yawing motion remains constant.

7. The drag and stability coefficients were obtained using data reduction techniques described in reference (b).

8. Tables II through VIII list the drag coefficients, slope of the normal force coefficients, and slope of the pitching moment coefficients both uncorrected and corrected to zero yaw for all of the SAMOS configurations tested. The slope of the damping moment coefficient uncorrected to zero yaw is also included. This coefficient was not corrected to zero yaw because of the high probable error and resultant scatter in the coefficient. However, the uncorrected data were plotted and a rough curve drawn through the points (Figure 5). The existence of any effect upon the dynamic stability coefficient with a variation of either the center of gravity location or the nose corner radius could not be inferred from the data obtained in this program.

9. The coefficients were corrected to zero yaw by using one of the following equations:

$$C_{D_0} = C_D - k_D \delta^2,$$

$$C_{M_{\alpha_0}} = C_{M_{\alpha}} - k_M \delta^2,$$

and

$$C_{N_{\alpha_0}} = C_{N_{\alpha}} - k_N \delta^2$$

where the factors k_D , k_M , and k_N were determined from a number of rounds within a given Mach number region.

CONFIDENTIAL
NAVWEPS Report 7389

Because of the limited number of models with a full-scale nose corner radius of one inch, the data obtained from these models were corrected to zero yaw by means of correction factors obtained from models with a full-scale nose corner radius of two inches. This was deemed justifiable since the scatter in the data from these configurations was larger than any systematic difference caused by the different nose corner radii.

10. Figure 6 is a plot of the drag coefficient against Mach number. It shows an increase in the drag coefficient with a decrease of the nose corner radius.

11. The plot of the slope of the normal force coefficient (Figure 7) indicates an increase in the coefficient with an increase in the nose corner radius. However, there is an overlapping of points for the two-inch and five-inch full-scale corner radius models caused by the scatter of the data.

12. Figure 8 is a plot of the slope of the pitching moment coefficient against Mach number. It is broken into two center of gravity groups. The group with a center of gravity location of approximately 35 percent of the length from the nose of the model illustrates an increase in the slope of the pitching moment coefficient with a decrease in the nose corner radius. This, along with the trend of the slope of the normal force coefficient, indicates a forward movement of the center of pressure with an increase in nose corner radius. Notice that as for the slope of the normal force coefficient, the data for the two-inch and five-inch corner radius models overlap. The other group of points seems to indicate just the opposite trend - an increase in the slope of the pitching moment coefficient with an increase in the nose corner radius. However, one explanation might be that the scatter in the data for the two-inch and for the five-inch full-scale corner radius models together with the 2.4 percent difference in the center of gravity location of the two types of models causes this apparent anomaly.

Conclusions

13. An increase in the drag coefficient with a decrease of the nose corner radius was observed on models of the SAMOS configuration.

14. The slope of the normal force coefficient decreased with a decrease in the nose corner radius. The slope of the

CONFIDENTIAL
NAVWEPS Report 7389

pitching moment coefficient increased with a decrease in the nose corner radius for a center of gravity location from the nose of approximately 35 percent of the length. Therefore, from the experimental data, it is observed that the center of pressure moves rearward as the nose corner radius is decreased.

15. No measurable effect of center of gravity location, nose corner radius, or angle of attack could be observed upon the dynamic stability of the SAMOS models investigated.

CONFIDENTIAL
NAVWEPS Report 7389

References

- (a) May, A., and Williams, F.J., "Free-Flight Ranges at the Naval Ordnance Laboratory," NavOrd Report 4063 (1955)
- (b) Murphy, C. H., "Data Reduction for the Free-Flight Spark Ranges," BRL Report No. 900 (1954)

TABLE I
AVERAGE WEIGHTS AND MOMENTS OF INERTIA OF SAMOS MODELS

DRAWING NO.	1831	1831-5	1844	2304-11	2304-7	2205-5	2304-9
	RD. 3846	Rest of RD's.	RD. 3849	Rest of RD's.			
Weight (Grams)	22.288	37.974	37.996	10.871	19.242	14.144	14.045
I_A (Gram-In. ²)	1.538	2.622	2.631	0.480	0.849	0.387	0.383
I_B (Gram-In. ²)	1.847	3.124	3.122	0.584	1.01	0.475	0.470

CONFIDENTIAL

CONFIDENTIAL
 NAVWEPS Report 7389
 DRAG AND STABILITY DATA FOR
 SAMOS MODELS (DRAWING NO. 1831)

TABLE II

ROUND	3803	3802	3796	3846
Max. Full-Scale Nose Corner Rad. (In.)	1	1	1	1
M	5.121	5.418	5.664	6.247
δ^2 (Deg.) ²	4000	136	4170	25
$Re_D \times 10^{-6}$	2.211	2.348	1.278	1.429
C_D	1.273	1.443	1.366	1.526
P.E. (\pm)	.001	.003	.001	.001
C_{D_0}	*	1.493	*	1.535
P.E.y (Rad.) (+) P.E.s (In.) (-)				.004 .02
C_{M_α} /Deg.	-.0006	-.0013	-.0008	-.00119
P.E. (+) C_{M_α} /Deg.	*	-.0015	*	.00001 -.00123
C_{N_α} /Deg. P.E. (+) C_{N_α} /Deg.				-.010 .001 -.010
$C_{M_q} + C_M$ & P.E. (-)				-.7 .2
CP-CG (Cal.) CG_N (In.)	.395	.394	.394	.399
Length (In.)	.880	.880	.879	.880
Diameter (In.)	.749	.749	.749	.750
$\lambda_1 \times 10^3$ (1/Ft.)				.798
$\lambda_2 \times 10^3$ (1/Ft.)				+1.973

* These rounds were not corrected to zero yaw because of the high δ^2 . In this region, C_D and C_{M_α} cannot be assumed linear with δ^2 .

CONFIDENTIAL

CONFIDENTIAL

NAVWEPS Report 7

DRAG AND STABILITY DATA
SAMOS MODELS (DRAWING N)

TABLE IV

ROUND	3814	3814	3817	3814	3817	3823	38
Full-Scale Nose Corner Rad. (In.)	2	2	2	2	2	2	2
M	4.686	4.997	5.202	5.226	5.496	5.843	5.8
δ^2 (Deg.) ²	106	100	22	93	20	205	
$Re_D \times 10^{-6}$	1.599	1.705	1.455	1.783	1.537	1.468	1.6
C_D	1.425		1.520	1.465		1.146	1.5
P.E. (+)	.004		.003	.002		.004	.00
C_{D_0}	1.464		1.528	1.499		1.522	1.52
P.E.y (Rad.) (+)		.009			.006		
P.E.s (In.) (+)		.02			.009		
$C_{M\alpha}$ /Deg.		-.00117			-.00150		
P.E. (-)		.00001			.00001		
$C_{M\alpha_0}$ /Deg.		-.00135			-.00154		
$C_{N\alpha}$ /Deg.		-.0138			-.0118		
P.E. (-)		.0009			.0007		
$C_{N\alpha_0}$ /Deg.		-.0130			-.0116		
$C_{Mq} + C_{M\alpha}$		-.2			-.1		
P.E. (+)		.2			.2		
CP - CG (Cal.)		.085			.125		
CG_N (In.)	.316	.316	.314	.316	.314	.315	.31
Length (In.)	.703	.703	.701	.703	.701	.702	.70
Diameter (In.)	.600	.600	.600	.600	.600	.600	.60
$\lambda_1 \times 10^3$ (1/Ft.)		+1.285			+.913		
$\lambda_2 \times 10^3$ (1/Ft.)		+1.121			+2.034		

* This round was not corrected to zero yaw because of the high δ^2 . In this region, C_D and $C_{M\alpha}$ cannot be compared directly with other data.

** Not corrected to zero yaw because of high P.E., as compared to other $C_{N\alpha}$ data, and subsequent inaccuracy.

CONFIDENTIAL

CONFIDENTIAL

NAVWEPS Report 7389
 AG AND STABILITY DATA FOR
 S MODELS (DRAWING NO. 1844)



TABLE IV

3823	3817	3821	3823	3826	3819	3823	3849	3816
2	2	2	2	2	2	2	2	2
5.843	5.872	6.010	6.182	6.296	6.302	6.484	6.524	6.559
205	17	180	191	309	119	176	15	2990
1.1468	1.642	1.635	1.553	1.591	1.662	1.632	1.217	1.783
1.146	1.519	1.429		1.349	1.481	1.454	1.511	1.073
.004	.001	.002		.004	.001	.003	.001	.002
1.522	1.525	1.496		1.463	1.525	1.519	1.517	*
		.01	.01		.02		.01	
		.03	.02		.07		.06	
		-.00108	-.00118	-.0006	-.00128		-.00103	-.0007
		.00002	.00001		.00002		.00009	
		-.00140	-.00152	-.0012	-.00149		-.00106	*
		-.0111	-.0115		-.005		-.006	
		.0006	.0003		.006		.004	
		-.0097	-.0100		**		**	
		-.5	0		+.3		-.5	
		.4	.2		.4		1.7	
		.099	.103		.243		.168	
.315	.314	.314	.315	.313	.314	.315	.320	.316
.702	.701	.701	.702	.701	.701	.702	.695	.703
.600	.600	.600	.600	.600	.600	.600	.603	.600
		-.467	+1.452		+1.833		-.852	
		+.964	+1.210		+3.189		+2.306	

ion, C_D and $C_M\alpha$ cannot be assumed linear with δ^2 ,
 , and subsequent inaccuracy.

CONFIDENTIAL



DR
344)

3821	3823	3826	3819	3823	3849	3816	3834
------	------	------	------	------	------	------	------

2	2	2	2	2	2	2	2
6.010	6.182	6.296	6.302	6.484	6.524	6.559	7.136
180	191	309	119	176	15	2990	61
1.635	1.553	1.591	1.662	1.632	1.217	1.783	1.285
1.429		1.349	1.481	1.454	1.511	1.073	1.478
.002		.004	.001	.003	.001	.002	.001
1.496		1.463	1.525	1.519	1.517	*	1.501
.01	.01		.02		.01		.005
.03	.02		.07		.06		.02
-.00108	-.00118	-.0006	-.00128		-.00103	-.0007	-.00113
.00002	.00001		.00002		.00009		.00001
-.00140	-.00152	-.0012	-.00149		-.00106	*	-.00124
-.0111	-.0115		-.005		-.006		-.0099
.0006	.0003		.006		.004		.0009
-.0097	-.0100		**		**		-.0094
-.5	0		+.3		-.5		+.3
.4	.2		.4		1.7		.2
.099	.103		.243		.168		.114
.314	.315	.313	.314	.315	.320	.316	.315
.701	.702	.701	.701	.702	.695	.703	.702
.600	.600	.600	.600	.600	.603	.600	.600
-.467	+1.452		+1.833		-.852		+1.660
+.964	+1.210		+3.189		+2.306		+1.355

assumed linear with δ^2 .

y.

DRAG AND STABILITY DATA FOR
SAMOS MODELS (DRAWING NO. 1831 - 5)

TABLE III

ROUND	3820	3824	3820	3812	3808	3812	3811	3808	3808
Full-Scale Nose									
Corner Rad. (In.)	2	2	2	2	2	2	2	2	2
M	4.356	4.461	4.586	4.908	5.285	5.464	5.477	5.518	5.637
δ^2 (Deg.) ²	69	310	66	63	77	220	81	179	5.792
$Re_D \times 10^{-6}$	1.851	1.859	1.949	2.086	2.260	1.255	2.313	2.359	204
C_D	1.475	1.348	1.479	1.681	1.603	1.412	1.403	1.406	1.330
P.E. (+)	.007	.002	.006	.002	.001	.003	.003	.006	.006
C_{D_0}	1.501	1.463	1.502	1.509	1.484	1.478	1.478	1.478	1.478
P.E. γ (Rad.) (+)	.02	.006	.01	.006	.01	.01	.01	.007	.007
P.E.S (In.) (+)	.06	.06	.02	.02	.02	.02	.02	.02	.02
$C_{M\alpha}$ / Deg.	-0.00087	-0.00126	-0.00126	-0.00126	-0.00126	-0.00126	-0.00126	-0.00126	-0.00094
P.E. (+)	.00002	.00001	.00002	.00002	.00002	.00002	.00002	.00002	.00005
$C_{M\alpha}/\Delta\alpha_0$	-0.00143	-0.00138	-0.00143	-0.00143	-0.00143	-0.00143	-0.00143	-0.00143	-0.00132
$C_{N\alpha}$ / Deg.	-0.013	-0.0126	-0.013	-0.0126	-0.0126	-0.0126	-0.0126	-0.0126	-0.0134
P.E. (+)	.001	.0004	.001	.0004	.0004	.0009	.0009	.0007	.0007
$\tilde{N}\alpha_0$ / Deg.	-0.011	-0.0121	-0.011	-0.0121	-0.0121	-0.0109	-0.0109	-0.0117	-0.0117
$C_M + C_M\alpha$	-4	-3	-4	-3	-3	-2	-2	-2	-2
P.E. (+)	.5	.2	.5	.2	.2	.3	.3	.3	.3
CP CG (Gal.)	.066	.099	.066	.099	.099	.109	.109	.109	.070
CGN (In.)	.395	.395	.395	.395	.395	.395	.395	.395	.395
Length (In.)	.879	.879	.879	.879	.879	.880	.880	.880	.880
Diameter (In.)	.719	.719	.719	.719	.719	.750	.750	.750	.750
$\lambda_1 \times 10^3$ (1/ft.)	-1.16	+1.261	-1.16	+1.261	+1.261	+2.528	+2.528	+2.528	+2.528
$\lambda_2 \times 10^3$ (1/ft.)	+.933	+.528	+.933	+.528	+.528	+.693	+.693	+.693	+.693

CONFIDENTIAL
NAVWEPS Report 7389

CONFIDENTIAL

CONFIDENTIAL

DRAG AND STABILITY DATA FOR
SAMOS MODELS (DRAWING NO. 2304-11)

TABLE V

ROUND	3968	3970	3926	3924	3935	3928	4006	4065	4067
Full Scale Nose Corner Rad. (In.)	2	2	2	2	2	2	2	2	2
$M_{\frac{g}{2}}^2$ (Deg.) 2	4.706	4.777	5.131	5.158	5.186	5.271	5.897	7.240	7.343
$Re_D \times 10^{-6}$	44	147	174	1330	1370	634	77	162	245
Re_D	1.339	1.359	0.750	0.739	0.770	0.780	1.640	0.601	0.741
C_D	1.471	1.458	1.429	1.272	1.269	1.307	1.453	1.407	1.400
P.E. (\pm)	.001	.001	.001	*.001	*.001	.003	.001	.001	.002
C_{D_0}	1.487	1.512	1.493	*	*	1.542	1.481	1.467	1.491
$P.E.y \{Rad.\} \{\pm\}$.01	.006	.01	.03	.05	.01	.007	.01	.008
$P.E.s \{In.\} \{\pm\}$.01	.02	.01	.03	.03	.02	.02	.02	.01
$C_{M_\alpha}/Deg.$	-.00247	-.002625	-.00243	-.00284	-.00283	-.00275	-.00244	-.00246	-.00256
P.E. (\pm)	.00002	.000006	.00002	.00001	.00002	.00001	.00001	.00002	.00001
$C_{M_\alpha}/Deg.$	-.00248	-.002665	-.00248	*.00248	*.00248	-.00292	-.00246	-.00250	-.00263
$C_{N_\alpha}/Deg.$	-.011	-.012	-.0119	-.0258	-.0248	-.0167	-.012	-.012	-.012
P.E. (\pm)	.001	.001	.0007	.0009	.0006	.0007	.002	.001	.007
$C_{N_\alpha}/Deg.$	-.011	-.011	-.0105	*	*	-.0116	-.011	-.011	-.010
$C_{M_\alpha} + C_{M_{\alpha'}}$	-1.0	-.46	+.9	-.5	-.6	-.1	-.3	+.3	+.4
P.E. (\pm)	.3	.08	.3	.2	.3	.2	.2	.4	.3
CP-CG (Cal.)	.217	.219	.204	.110	.114	.164	.208	.201	.216
C_{GN} (In.)	.205	.205	.205	.205	.206	.206	.207	.207	.206
Length (In.)	.583	.583	.584	.584	.584	.584	.583	.584	.583
Diameter (In.)	.500	.500	.500	.500	.500	.500	.500	.500	.500
$\lambda_1 \times 10^3$ (1/Ft.)	.455	+2.062	+.142	-.597	-.123	+.932	+1.518	+1.461	
$\lambda_2 \times 10^3$ (1/Ft.)	-.236	+2.685	-.898	+.216	+1.055	+.859	+.028	+.518	

* These rounds were not corrected to zero yaw because of the high δ^2 . In this region, C_D , C_{M_α} , C_{N_α} cannot be assumed linear with δ^2 .

CONFIDENTIAL

NAVWEPS Report 7389

CONFIDENTIAL
 NAVWEPS Report 7389
 DRAG AND STABILITY DATA FOR
 SAMOS MODELS (DRAWING NO. 2205-5)

TABLE VI

ROUND	4074	4013	4071	4005
Full Scale Nose Corner Rad. (In.)	5	5	5	5
$\frac{M}{\delta}^2$ (Deg. ²)	5.336	5.512	5.624	6.119
$Re_D \times 10^{-6}$	31	51	9	192
	1.499	1.544	1.573	1.700
C_D	1.409	1.423	1.424	1.385
P.E. (\pm)	.001	.001	.001	.001
C_{D_0}	1.418	1.438	1.427	1.443
P.E.y{Rad.}(\pm)	.01	.004	.006	
P.E.s(In.)(\pm)	.02	.02	.01	
C_{M_α} /Deg.	-.00156	-.00144	-.00163	-.00151
P.E. (\pm)	.00003	.00001	.00002	.00004
$C_{M_{\alpha_0}}$ /Deg.	-.00157	-.00146	-.00163	-.00158
C_{N_α} /Deg.	-.013	-.0114	-.010	
P.E. (\pm)	.001	.0009	.002	
$C_{N_{\alpha_0}}$ /Deg.	-.013	-.0110	-.010	
$C_M + C_{M_\alpha}$	+.4	-.1	+.1	
P.E. (\pm)	.8	.2	.5	
CP-CG (Cal.)	.121	.126	.171	
CG _N (In.)	.249	.248	.249	.247
Length (In.)	.585	.583	.585	.583
Diameter (In.)	.501	.500	.500	.500
$\lambda_1 \times 10^3$ {1/Ft.}	+2.434	+.351	+.216	
$\lambda_2 \times 10^3$ {1/Ft.}	+1.192	+1.784	+2.708	

CONFIDENTIAL

CONFIDENTIAL
 NAVWEPS Report 7389
 DRAG AND STABILITY DATA FOR
 SAMOS MODELS (DRAWING NO. 2304 - 7)

TABLE VII

ROUND	3967	3964	3969	3966	3954
Full-Scale Nose Corner Rad. (In.)	5	5	5	5	5
$\frac{M}{\delta}^2$ (Deg. 2)	4.793	5.199	5.206	5.246	5.955
$Re_D \times 10^{-6}$	75	114	3	14	372
C_D	1.346	1.460	1.481	1.469	0.890
P.E. (\pm)	1.4243	1.398	1.445	1.432	1.321
C_{D_0}	.0004	.001	.001	.001	.001
P.E.y(Rad.) (\pm)	1.4468	1.432	1.446	1.436	1.433
P.E.s(In.) (\pm)	.01	.01	.006	.008	.008
C_{M_α} /Deg.	.01	.01	.01	.01	.01
P.E. (\pm)	-.00250	-.00233	-.00250	-.00255	-.002406
$C_{M_{\alpha_0}}$ /Deg.	.00002	.00004	.00005	.00003	.000006
C_{N_α} /Deg.	-.00252	-.00237	-.00250	-.00255	-.002525
P.E. (\pm)	-.0136	-.011	-.013	-.012	-.0147
$C_{N_{\alpha_0}}$ /Deg.	.0006	.004	.009	.004	.0006
P.E. (\pm)	-.0130	-.010	-.013	-.012	-.0120
$C_{M_q} + C_{M_{\alpha_0}}$	-.1	+.3	-2.1	-.4	+.1
P.E. (\pm)	.2	.6	.7	.4	.1
CP-CG (Cal.)	.184	.209	.198	.204	.164
CG_N (In.)	.205	.206	.206	.206	.206
Length (In.)	.583	.584	.583	.584	.583
Diameter (In.)	.500	.500	.500	.500	.500
$\lambda_1 \times 10^3$ (1/Ft.)	+1.223	+.835	-1.683	+.420	+.465
$\lambda_2 \times 10^3$ (1/Ft.)	+1.570	+4.386	-7.575	+.738	+1.343

CONFIDENTIAL

CONFIDENTIAL
DRAG AND STABILITY DATA FOR
SAMOS MODELS (DRAWING NO. 2304-9)

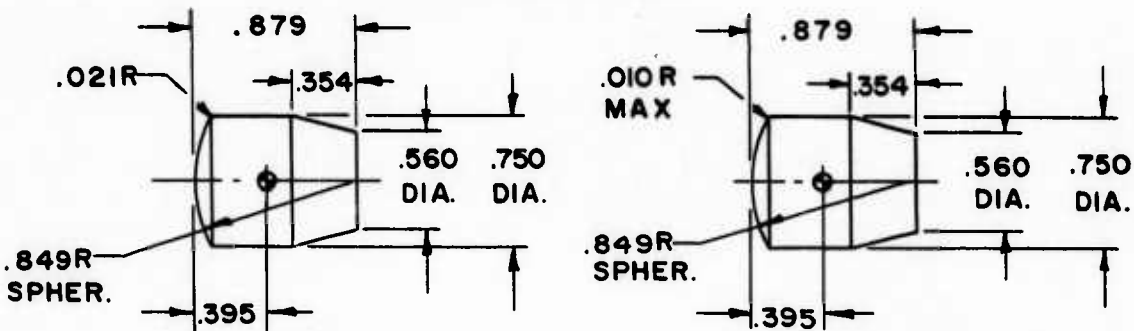
TABLE VIII

ROUND	3961	3955	4007	4064	4010	4066	4068
Full Scale Nose Corner Rad. (In.)	8	8	8	8	8	8	8
M_{∞}^2 (Deg 2) $Re_D \times 10^{-6}$	5.372 1.97 1.514	6.200 332 0.939	6.224 149 1.738	6.392 305 1.782	6.932 230 0.764	7.285 372 0.678	7.389 358 0.665
C_D	1.315	1.287	1.337	1.324	1.34	1.298	1.279
P.E. (\pm)	.001	.001	.001	.001	.07	.001	.003
C_{D_0}	1.358	1.360	1.370	1.391	1.39	1.380	1.358
P.E.Y (Rad.) (\pm) P.E.s (In.) (\pm)	.02 .01	.01 .01	.01 .02	.01 .02			.03 .04
$C_{M_\alpha}/\text{Deg.}$ P.E. (\pm)	-.00235 .00001 -.00237	-.002244 .00009 -.002279	-.00227 .00001 -.00229	-.0023 -.0023	-.00238 -.00240	-.0023 -.0023	-.00233 .0004 -.00237
$C_{M_{\alpha_0}}/\text{Deg.}$							
$C_{N_\alpha}/\text{Deg.}$ P.E. (\pm)	-.0139 .0006 -.0139	-.0149 .0006 -.0148	-.0137 .0008 -.0137				-.013 .003 -.013
$C_{N_{\alpha_0}}/\text{Deg.}$							
$C_{M_q} + C_{M_\alpha}$ P.E. (\pm)	+.3 .2	-.2 .2	-.3 .2			0	1
CP-CG (cal.)	.169	.150	.166				.176
CG _N (In.)	.206	.207	.207				.207
Length (In.)	.582	.583	.583				.583
Diameter (In.)	.500	.500	.500				.500
$\lambda_1 \times 10^3$ (1/ft.)	+2.818	+.252	+1.122				+.594
$\lambda_2 \times 10^3$ (1/ft.)	+2.124	+.686	+.242				+.652

CONFIDENTIAL

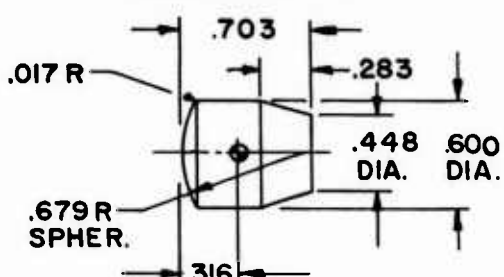
CONFIDENTIAL
NAVWEPS Report 7389

CONFIDENTIAL
NAVWEPS Report 7389

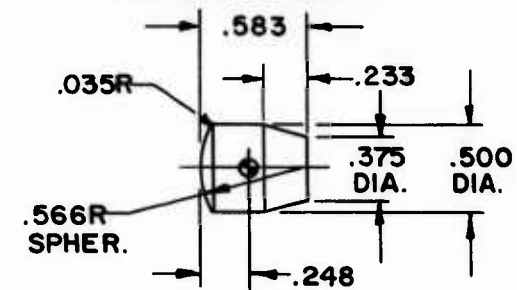


DWG. NO. 1831-5

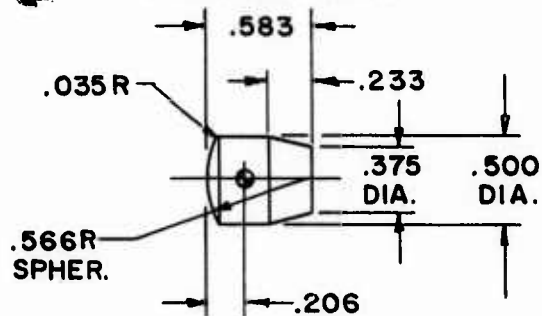
DWG. NO. 1831



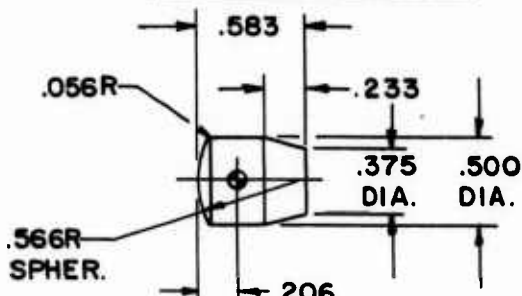
DWG. NO. 1844



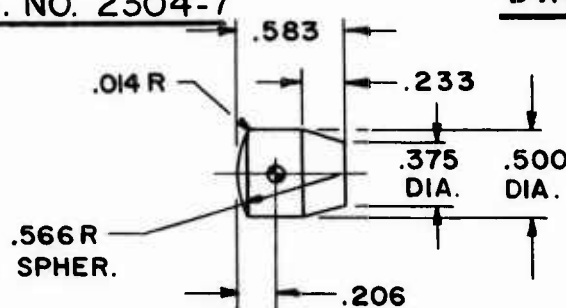
DWG. NO. 2205-5



DWG. NO. 2304-7



DWG. NO. 2304-9

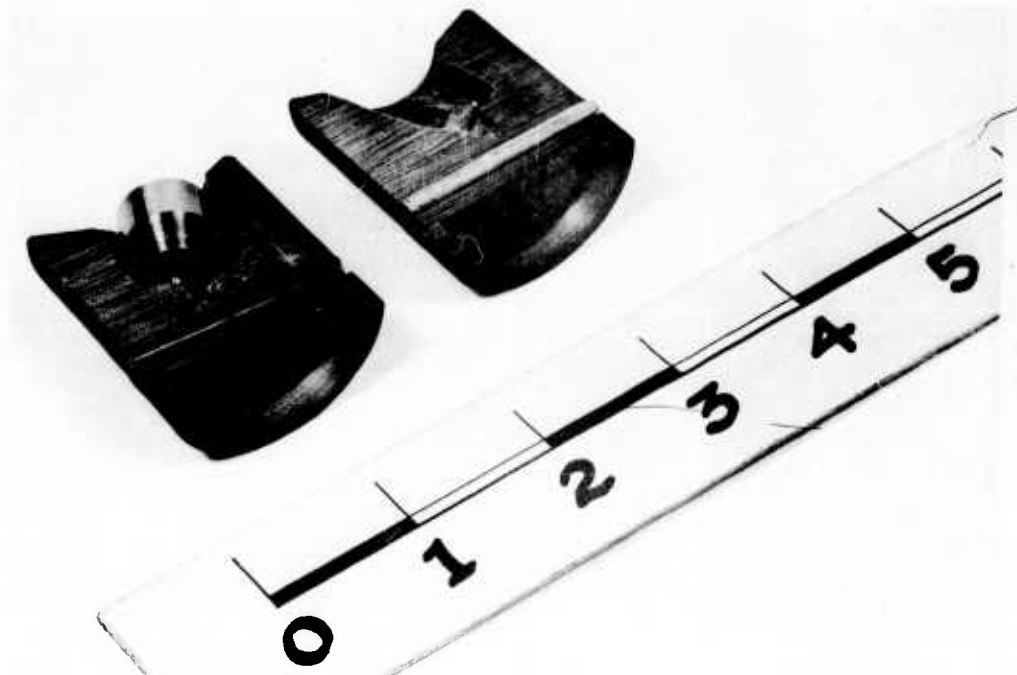


DWG. NO. 2304-11

NOTE:
DIMENSIONS ARE IN
INCHES.

FIG. I SAMOS MODELS
CONFIDENTIAL

CONFIDENTIAL
NAVWEPS REPORT 7389



25° POWDER GUN SABOT AND MODEL



0° GAS GUN SABOT AND MODEL

FIG.2 - SAMOS MODELS AND SABOTS

CONFIDENTIAL

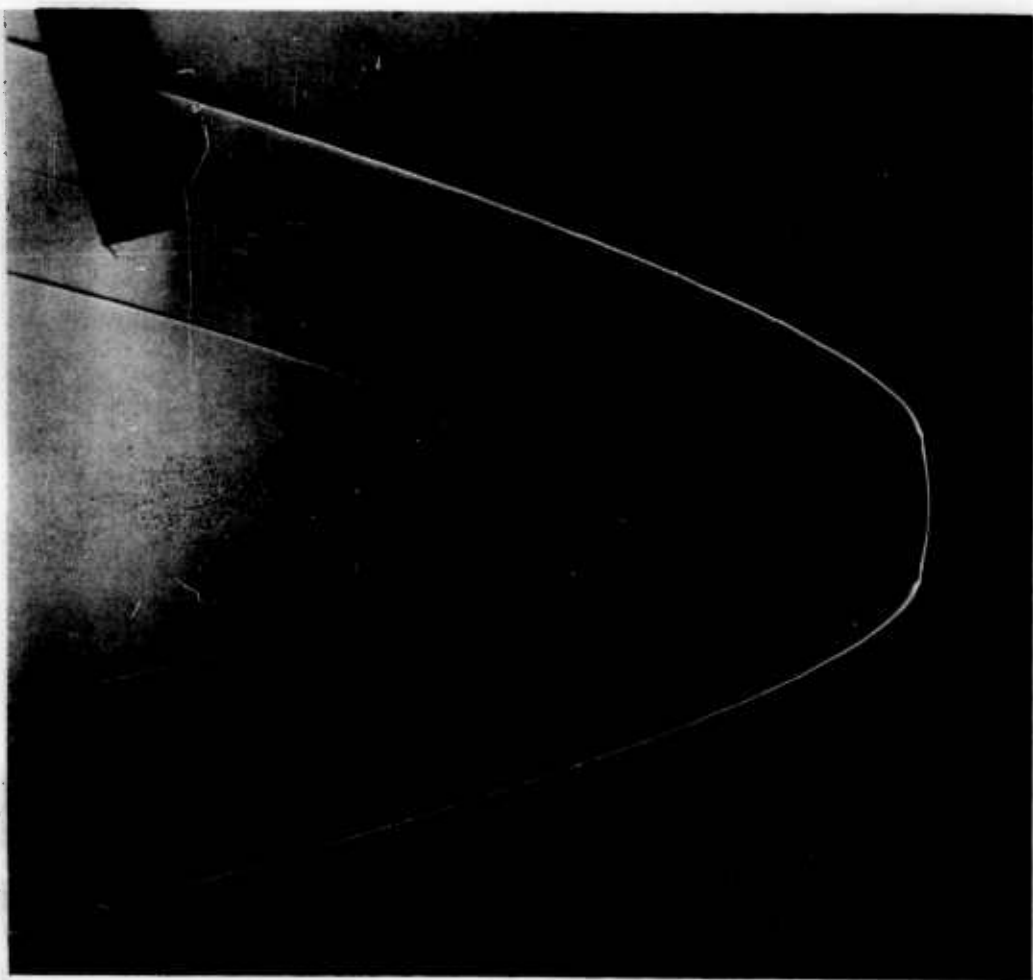
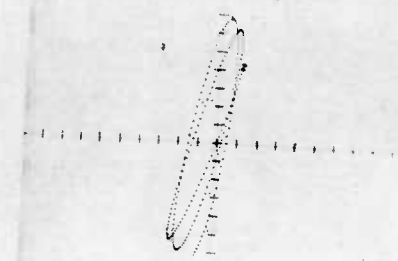


FIG. 3 SHADOWGRAPH PRINT OF SAMOS MODEL
WITH A FULL-SCALE NOSE CORNER
RADIUS OF TWO INCHES (1831-5),
ROUND 3812, M= 4.94

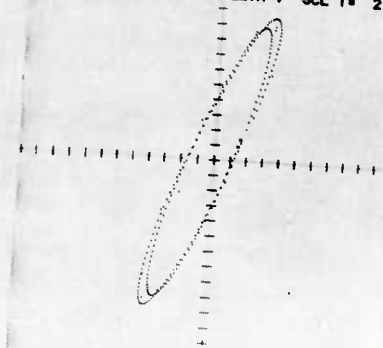
CONFIDENTIAL
NAVWEPS REPORT 7389

ROUND 3917 ZETA H VS-ZETA V SCL I = 1 D



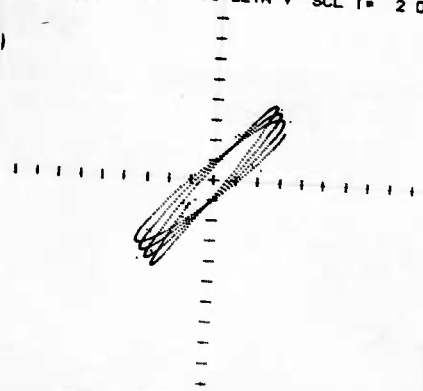
$CG_N = 0.527$ CAL.
INITIAL LAUNCH ANGLE = 0°

ROUND 3923 ZETA H VS-ZETA V SCL I = 2 D



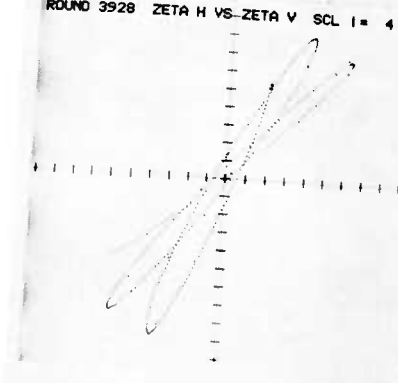
$CG_N = 0.527$ CAL.
INITIAL LAUNCH ANGLE = 15°

ROUND 3968 ZETA H VS-ZETA V SCL I = 2 D



$CG_N = 0.412$ CAL.
INITIAL LAUNCH ANGLE = 0°

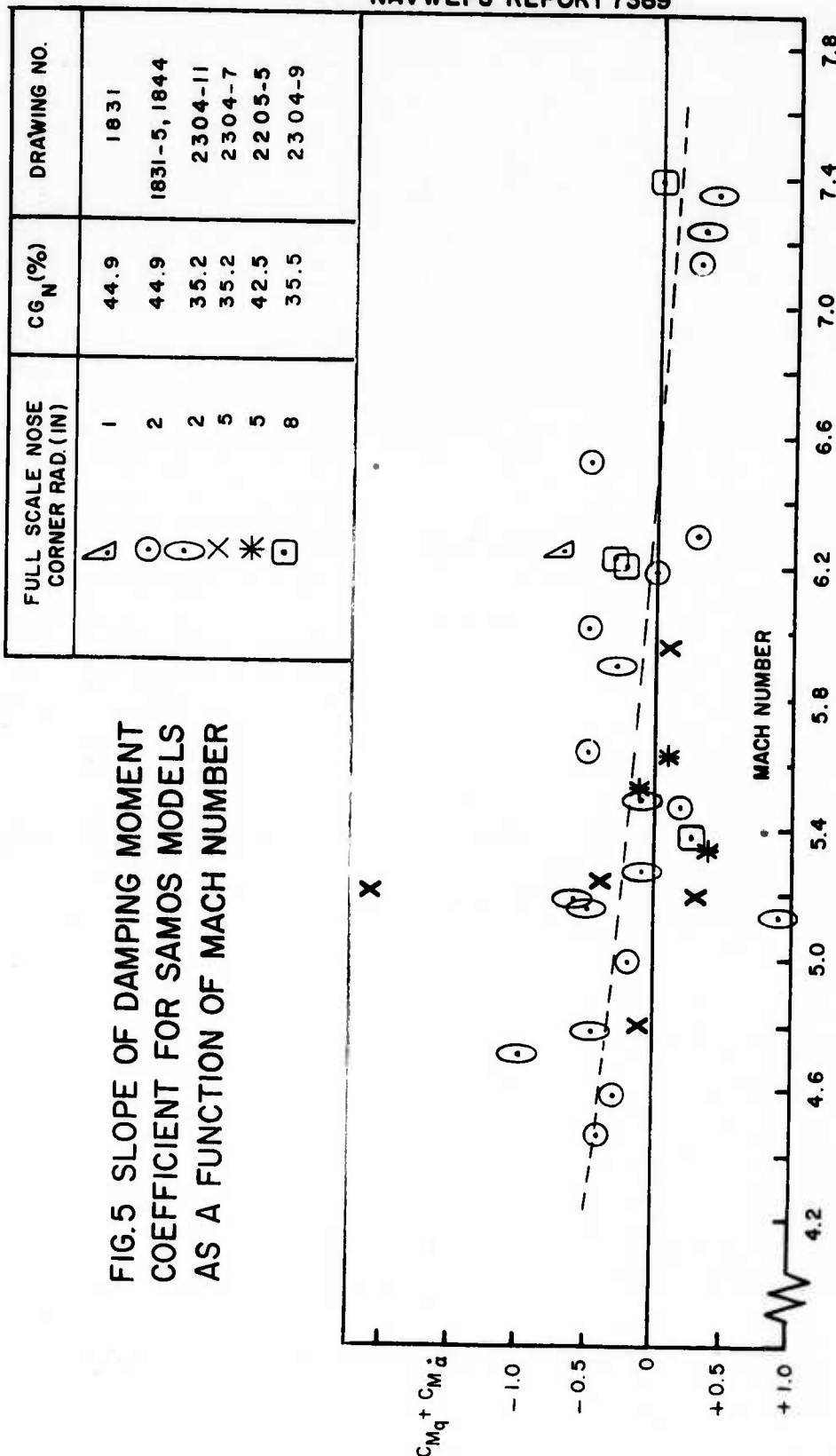
ROUND 3928 ZETA H VS-ZETA V SCL I = 4 D



$CG_N = 0.412$ CAL.
INITIAL LAUNCH ANGLE = 25°

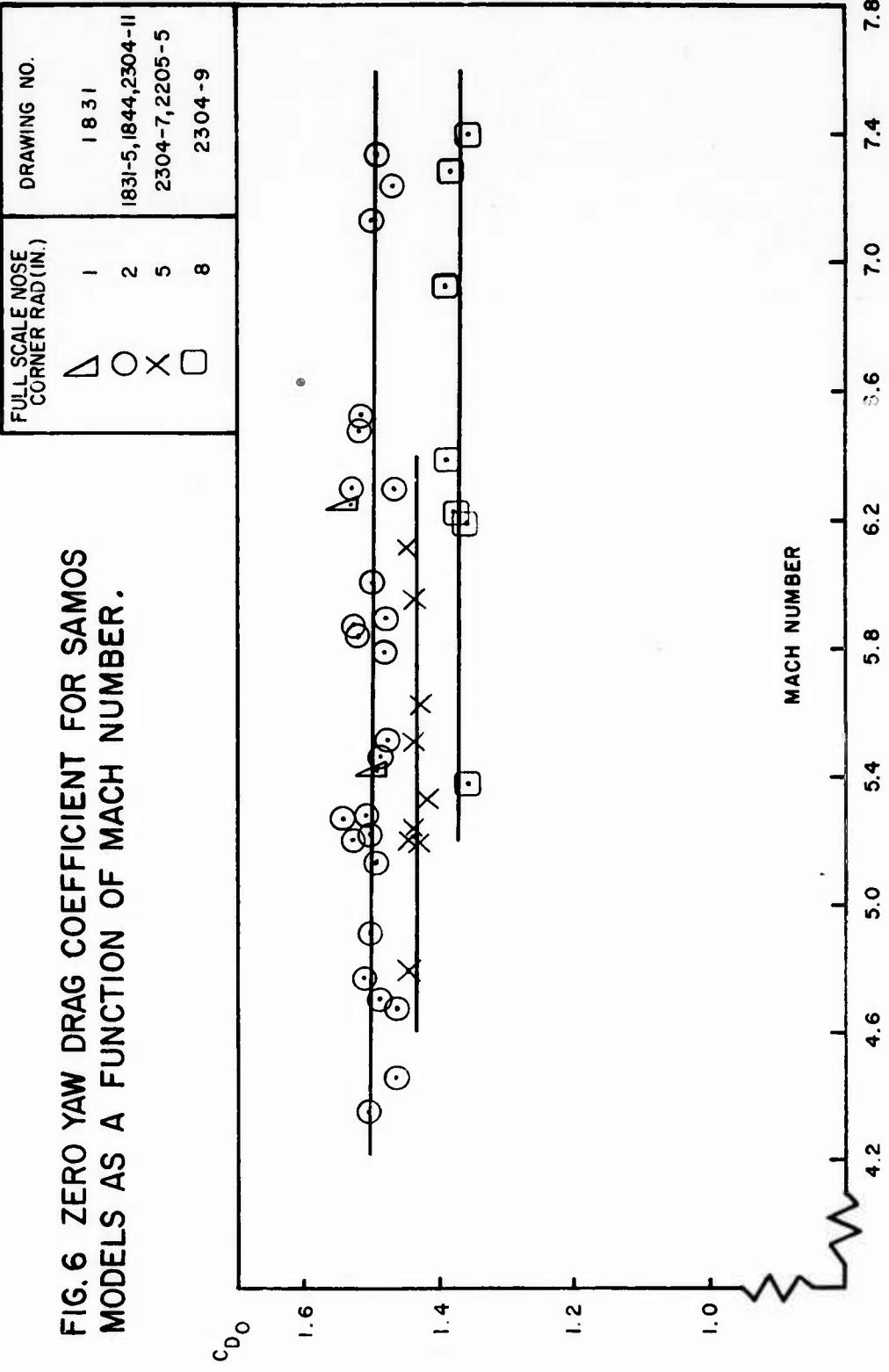
FIG.4 - COMPLEX ANGLE OF ATTACK PLOTS FOR SAMOS MODELS

CONFIDENTIAL

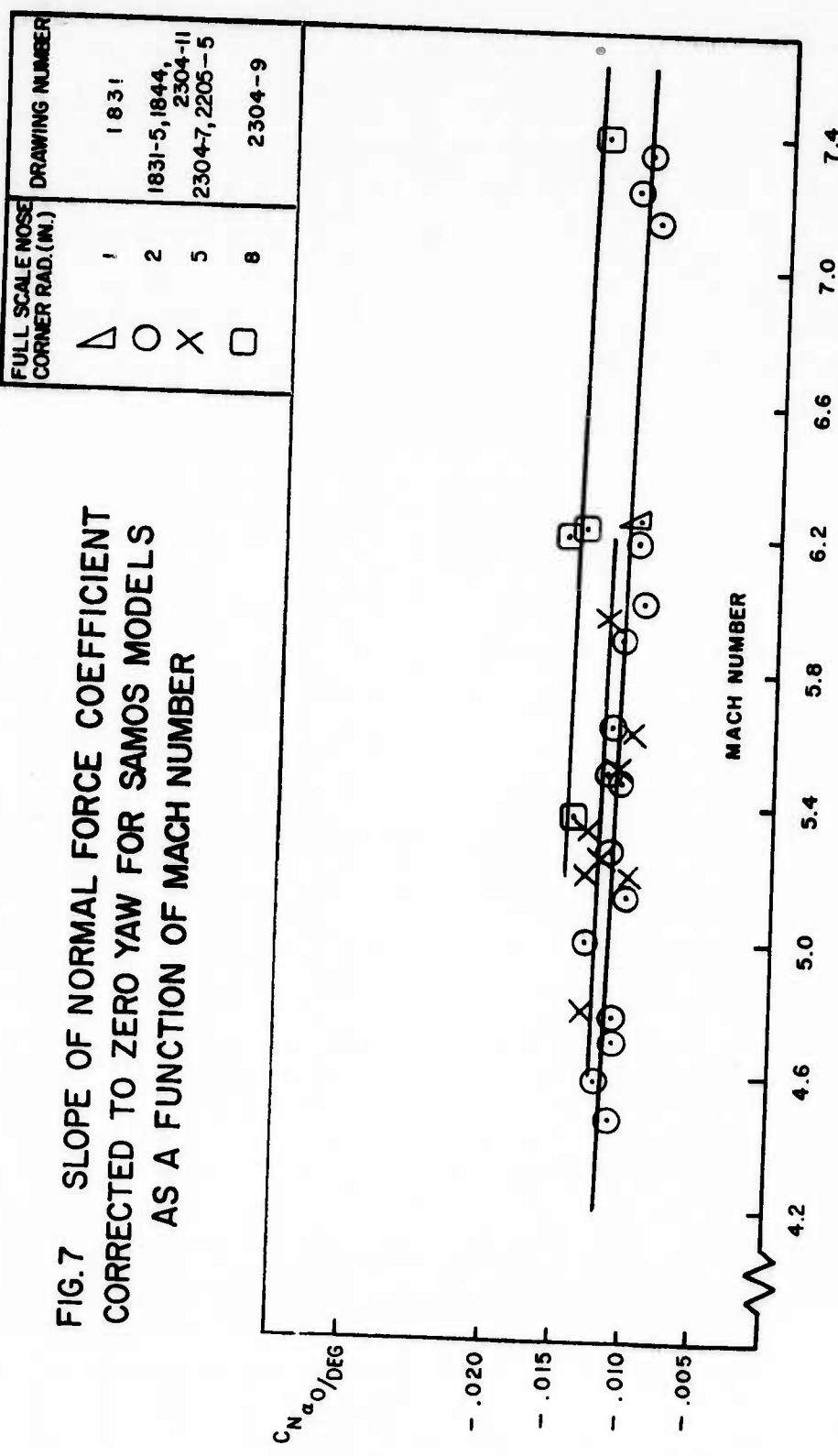


CONFIDENTIAL

CONFIDENTIAL
NAVWEPS REPORT 7389



CONFIDENTIAL

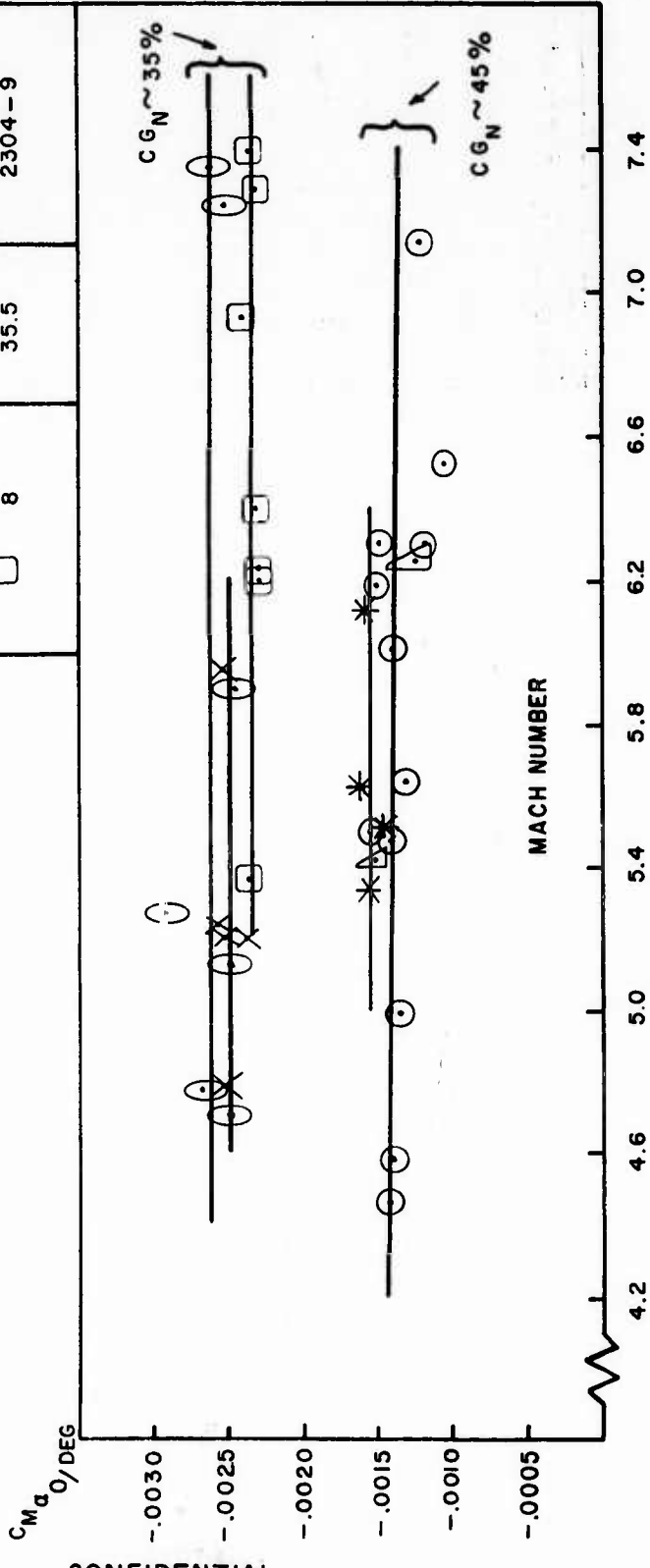


CONFIDENTIAL

FULL SCALE NOSE CORNER RAD. (IN.) CGN (%) DRAWING NUMBER

FULL SCALE NOSE CORNER RAD. (IN.)	CGN (%)	DRAWING NUMBER
△ 1	44.9	1831
○ 2	44.9	1831-5, 1844
○ 2	35.2	2304-11
× 5	35.2	2304-7
* 5	42.5	2205-5
□ 8	35.5	2304-9

FIG. 8 SLOPE OF PITCHING MOMENT COEFFICIENT CORRECTED TO ZERO YAW FOR SAMOS MODELS AS A FUNCTION OF MACH NUMBER.



CONFIDENTIAL

External Distribution List

<u>No. of Copies</u>		<u>No. of Copies</u>	
1	Chief Bureau of Naval Weapons Department of the Navy Washington 25, D. C. Attn: DLI-3	10	ASTIA Document Service Center Arlington Hall Station Arlington 12, Virginia
1	Commander U. S. Naval Ordnance Test Station China Lake, California Attn: Technical Lib.	1	NASA High Speed Flight Sta. Edwards Air Force Base California
2	Officer in Charge Naval Weapons Laboratory Dahlgren, Virginia Attn: Technical Lib.	1	Commander, AEDC Tullahoma, Tennessee Attn: Technical Lib.
1	Office of the Assistant Secretary of Defense (R and D) Room 3E 1065 The Pentagon Washington 25, D. C. Attn: Technical Lib.	12	Commanding Officer Office of Naval Research Branch Office Box 39, Navy 100 Fleet Post Office New York, New York
1	Chief, AFSWP Washington 25, D. C. Attn: Document Library Branch	1	NASA Ames Research Center Moffett Field, Calif. Attn: Librarian
2	Commander, WADC Wright-Patterson AF Base Ohio Attn: WCOSI-3	2	NASA Langley Research Center Langley Field Hampton, Virginia Attn: Librarian
1	Director Aberdeen Proving Ground Maryland Attn: Tech. Info. Br.	1	NASA Lewis Research Center 21000 Brookpark Road Cleveland 35, Ohio Attn: Librarian
1	Attn: Ballistics Res. Lab.		

CONFIDENTIAL
NAVWEPS Report 7389

No. of
Copies

1 NASA
 1512 H Street, N.W.
 Washington 25, D. C.

 Director of Intelligence
 Headquarters, USAF
 Washington 25, D. C.
1 Attn: AFOIN-3B

 Lockheed Missile and Space Division
 Department 6261
 Building 104
 Sunnyvale, California
2 Attn: Mr. Val Paline

 AVCO Corporation
 Research and Advanced Development Division
 201 Lowell Street
 Wilmington, Massachusetts
2 Attn: Mr. J. H. Grimes, Jr.

2 AFBMD (ARDC)
 U. S. Air Force
 Air Force Unit Post Office
 Los Angeles 45, California

CONFIDENTIAL

- Naval Ordnance Laboratory, White Oak, Md.
(NAVWEPS report 7389)
DRAG AND STABILITY DATA FOR SEVERAL SAMOS
CONFIGURATIONS OBTAINED FROM FREE-FLIGHT
MODEL FIRINGS (C), by Leonard E. Crogan.
3 April 1961. 5p. tables, diagrs. (Bal-
listic research report 39). CONFIDENTIAL
Firings of several Samos configurations
were conducted in the Naval Ordnance Labora-
tory pressurized ballistics range no. 3.
The configurations differed in nose corner
radius only. It was observed that with a de-
crease in the nose corner radius, the drag
coefficient increased, the slope of the nor-
mal force coefficient decreased, and the
slope of the pitching moment coefficient in-
creased. From these experimental data, it
was concluded that a decrease in the nose
corner radius resulted in a rearward move-
ment of the center of pressure.
Abstract card is confidential
1. Satellites - Samos
2. Satellites - Aerodynamics -
3. Satellites - Wind tunnel tests
Title I.
II. Crogan, Leonard E.
III. Series
- Naval Ordnance Laboratory, White Oak, Md.
(NAVWEPS report 7389)
DRAG AND STABILITY DATA FOR SEVERAL SAMOS
CONFIGURATIONS OBTAINED FROM FREE-FLIGHT
MODEL FIRINGS (C), by Leonard E. Crogan.
3 April 1961. 5p. tables, diagrs. (Bal-
listic research report 39). CONFIDENTIAL
Firings of several Samos configurations
were conducted in the Naval Ordnance Labora-
tory pressurized ballistics range no. 3.
The configurations differed in nose corner
radius only. It was observed that with a de-
crease in the nose corner radius, the drag
coefficient increased, the slope of the nor-
mal force coefficient decreased, and the
slope of the pitching moment coefficient in-
creased. From these experimental data, it
was concluded that a decrease in the nose
corner radius resulted in a rearward move-
ment of the center of pressure.
Abstract card is confidential
1. Satellites - Samos
2. Satellites - Aerodynamics -
3. Satellites - Wind tunnel tests
Title I.
II. Crogan, Leonard E.
III. Series
- Naval Ordnance Laboratory, White Oak, Md.
(NAVWEPS report 7389)
DRAG AND STABILITY DATA FOR SEVERAL SAMOS
CONFIGURATIONS OBTAINED FROM FREE-FLIGHT
MODEL FIRINGS (C), by Leonard E. Crogan.
3 April 1961. 5p. tables, diagrs. (Bal-
listic research report 39). CONFIDENTIAL
Firings of several Samos configurations
were conducted in the Naval Ordnance Labora-
tory pressurized ballistics range no. 3.
The configurations differed in nose corner
radius only. It was observed that with a de-
crease in the nose corner radius, the drag
coefficient increased, the slope of the nor-
mal force coefficient decreased, and the
slope of the pitching moment coefficient in-
creased. From these experimental data, it
was concluded that a decrease in the nose
corner radius resulted in a rearward move-
ment of the center of pressure.
Abstract card is confidential
1. Satellites - Samos
2. Satellites - Aerodynamics -
3. Satellites - Wind tunnel tests
Title I.
II. Crogan, Leonard E.
III. Series
- Naval Ordnance Laboratory, White Oak, Md.
(NAVWEPS report 7389)
DRAG AND STABILITY DATA FOR SEVERAL SAMOS
CONFIGURATIONS OBTAINED FROM FREE-FLIGHT
MODEL FIRINGS (C), by Leonard E. Crogan.
3 April 1961. 5p. tables, diagrs. (Bal-
listic research report 39). CONFIDENTIAL
Firings of several Samos configurations
were conducted in the Naval Ordnance Labora-
tory pressurized ballistics range no. 3.
The configurations differed in nose corner
radius only. It was observed that with a de-
crease in the nose corner radius, the drag
coefficient increased, the slope of the nor-
mal force coefficient decreased, and the
slope of the pitching moment coefficient in-
creased. From these experimental data, it
was concluded that a decrease in the nose
corner radius resulted in a rearward move-
ment of the center of pressure.
Abstract card is confidential

Naval Ordnance Laboratory, White Oak, Md.
(NAVWEPS report 7389)
DRAG AND STABILITY DATA FOR SEVERAL SAMOS
CONFIGURATIONS OBTAINED FROM FREE-FLIGHT
MODEL FIRINGS (C), by Leonard E. Crogan.
3 April 1961. 5p. tables, diags. (Bal-
listic research report 39). CONFIDENTIAL
Firings of several Samos configurations
were conducted in the Naval Ordnance Labora-
tory pressurized ballistics range no. 3.
The configurations differed in nose corner
radius only. It was observed that with a de-
crease in the nose corner radius, the drag
coefficient increased, the slope of the nor-
mal force coefficient decreased, and the
slope of the pitching moment coefficient in-
creased. From these experimental data, it
was concluded that a decrease in the nose
corner radius resulted in a rearward move-
ment of the center of pressure.
Abstract card is confidential

1. Satellites
- Samos
2. Satellites -
Aerodynamics
3. Satellites -
Wind tunnel
tests
Title
I.
II.
III. Series
Leonard E.
Crogan,
Leonard E.
Series

Naval Ordnance Laboratory, White Oak, Md.
(NAVWEPS report 7389)
DRAG AND STABILITY DATA FOR SEVERAL SAMOS
CONFIGURATIONS OBTAINED FROM FREE-FLIGHT
MODEL FIRINGS (C), by Leonard E. Crogan.
3 April 1961. 5p. tables, diags. (Bal-
listic research report 39). CONFIDENTIAL
Firings of several Samos configurations
were conducted in the Naval Ordnance Labora-
tory pressurized ballistics range no. 3.
The configurations differed in nose corner
radius only. It was observed that with a de-
crease in the nose corner radius, the drag
coefficient increased, the slope of the nor-
mal force coefficient decreased, and the
slope of the pitching moment coefficient in-
creased. From these experimental data, it
was concluded that a decrease in the nose
corner radius resulted in a rearward move-
ment of the center of pressure.
Abstract card is confidential

Naval Ordnance Laboratory, White Oak, Md.
(NAVWEPS report 7389)
DRAG AND STABILITY DATA FOR SEVERAL SAMOS
CONFIGURATIONS OBTAINED FROM FREE-FLIGHT
MODEL FIRINGS (C), by Leonard E. Crogan.
3 April 1961. 5p. tables, diags. (Bal-
listic research report 39). CONFIDENTIAL
Firings of several Samos configurations
were conducted in the Naval Ordnance Labora-
tory pressurized ballistics range no. 3.
The configurations differed in nose corner
radius only. It was observed that with a de-
crease in the nose corner radius, the drag
coefficient increased, the slope of the nor-
mal force coefficient decreased, and the
slope of the pitching moment coefficient in-
creased. From these experimental data, it
was concluded that a decrease in the nose
corner radius resulted in a rearward move-
ment of the center of pressure.
Abstract card is confidential

1. Satellites
- Samos
2. Satellites -
Aerodynamics
3. Satellites -
Wind tunnel
tests
Title
I.
II.
III. Series
Leonard E.
Crogan,
Leonard E.
Series

Naval Ordnance Laboratory, White Oak, Md.
(NAVWEPS report 7389)
DRAG AND STABILITY DATA FOR SEVERAL SAMOS
CONFIGURATIONS OBTAINED FROM FREE-FLIGHT
MODEL FIRINGS (C), by Leonard E. Crogan.
3 April 1961. 5p. tables, diags. (Bal-
listic research report 39). CONFIDENTIAL
Firings of several Samos configurations
were conducted in the Naval Ordnance Labora-
tory pressurized ballistics range no. 3.
The configurations differed in nose corner
radius only. It was observed that with a de-
crease in the nose corner radius, the drag
coefficient increased, the slope of the nor-
mal force coefficient decreased, and the
slope of the pitching moment coefficient in-
creased. From these experimental data, it
was concluded that a decrease in the nose
corner radius resulted in a rearward move-
ment of the center of pressure.
Abstract card is confidential

UNCLASSIFIED

UNCLASSIFIED